Journal of Molecular Graphics and Modelling 28 (2009) 162–169

Contents lists available at ScienceDirect

Journal of Molecular Graphics and Modelling

journal homepage: www.elsevier.com/locate/JMGM

Docking and molecular dynamics studies toward the binding of new natural phenolic marine inhibitors and aldose reductase

Zhiguo Wang [a,c], Baoping Ling [b], Rui Zhang [a,c], Yourui Suo [a], Yongjun Liu [a,b,*], Zhangyu Yu [b], Chengbu Liu [b,**]

[a] Northwest Institute of Plateau Biology, Chinese Academy of Sciences, Xining, Qinghai 810001, China
[b] School of Chemistry and Chemical Engineering, Shandong University, Jinan, Shandong 250100, China
[c] Graduate University of Chinese Academy of Science, Beijing 10049, China

ARTICLE INFO

Article history:
Received 17 March 2009
Received in revised form 5 June 2009
Accepted 13 June 2009
Available online 21 June 2009

Keywords:
Phenolic ARIs
Aldose reductase
Molecular docking
Dynamics
Inhibition

ABSTRACT

Phenolic marine natural product is a kind of new potential aldose reductase inhibitors (ARIs). In order to investigate the binding mode and inhibition mechanism, molecular docking and dynamics studies were performed to explore the interactions of six phenolic inhibitors with human aldose reductase (*h*ALR2). Considering physiological environment, all the neutral and other two ionized states of each phenolic inhibitor were adopted in the simulation. The calculations indicate that all the inhibitors are able to form stable hydrogen bonds with the *h*ALR2 active pocket which is mainly constructed by residues TYR48, HIS110 and TRP111, and they impose the inhibition effect by occupying the active space. In all inhibitors, only La and its two ionized derivatives La_ion1 and La_ion2, in which neither of the ortho-hydrogens of 3-hydroxyl is substituted by Br, bind with *h*ALR2 active residues using the terminal 3-hydroxyl. While, all the other inhibitors, at least one of whose ortho-sites of 3- and 6-hydroxyls are substituted by Br substituent which take much electron-withdrawing effect and steric hindrance, bind with *h*ALR2 through the lactone group. This means that the Br substituent can effectively regulate the binding modes of phenolic inhibitors. Although the lactone bound inhibitors have relatively high RMSD values, our dynamics study shows that both binding modes are of high stability. For each inhibitor molecule, the ionization does not change its original binding mode, but it does gradually increase the binding free energy, which reveals that besides hydrogen bonds, the electrostatic effect is also important to the inhibitor–*h*ALR2 interaction.

1. Introduction

Aldose reductase (alditol/$NADP^+$ oxidoreductase, EC 1.1.1.21, ALR2), belonged to the aldo-keto aldose superfamily, is the first enzyme of the polyol pathway. X-ray crystallographic studies on both porcine and human aldose reductases have shown that they belong to the $(\beta/\alpha)_8$ barrel class of enzymes and the coenzyme NADPH binds at the C-terminal end of the β barrel (Fig. 1) [1,2]. This enzyme catalyzes the reduction of D-glucose to D-sorbitol with concomitant conversion of NADPH to $NADP^+$, and the D-sorbitol is subsequently oxidized to D-fructose by sorbitol dehydrogenase (L-iditol: NAD^+, 5-oxidoreductase, EC 1.1.1.14, SD) [3,4]. Under hyperglycemia environment, ARL2 is highly activated, resulting in glucose metabolism rate increasing by 2–4 times, while, sorbitol-dehydrogenase dependent sorbitol has a common metabolism rate and poor penetration through cellular membranes. This leads to severe accumulation of sorbitol, which in turn initiates a cascade of events that cause the development of long-term diabetic complications, such as neuropathy, nephropathy, retinopathy, cataract, and cardio-vascular disease [3–7]. Inhibition of ALR2 is therefore proved to be a useful therapeutic strategy to prevent the onset or, at least, delay the progression and the deterioration of diabetic complications [7,8].

Many compounds have been shown to inhibit ALR2 effectively. Although chemically different, they all share common structural features, represented by a polar region with the function of anchoring inhibitor to the active pocket through hydrogen bonds and a generally wide lipophilic area used to bind to the highly plastic specialty pocket through hydrophobic interactions [9–11]. Currently known orally active ARIs belong to two main chemical classes: (i) carboxylic acid derivatives, such as Epalrestat and Tolrestat and (ii) spiro-hydantoins, such as Sorbinil and Fidarestat (Fig. 2) [7,12]. In vitro, carboxylic acids and spiro-hydantoins show

* Corresponding author at: School of Chemistry and Chemical Engineering, Shandong University, No. 27 Shan Da Nan Lu, Jinan, Shandong 250100, China. Fax: +86 531 885 644 64.
** Corresponding author. Fax: +86 531 885 644 64.
E-mail address: yongjunliu_1@sdu.edu.cn (C. Liu).

1093-3263/$ – see front matter © 2009 Elsevier Inc. All rights reserved.
doi:10.1016/j.jmgm.2009.06.003

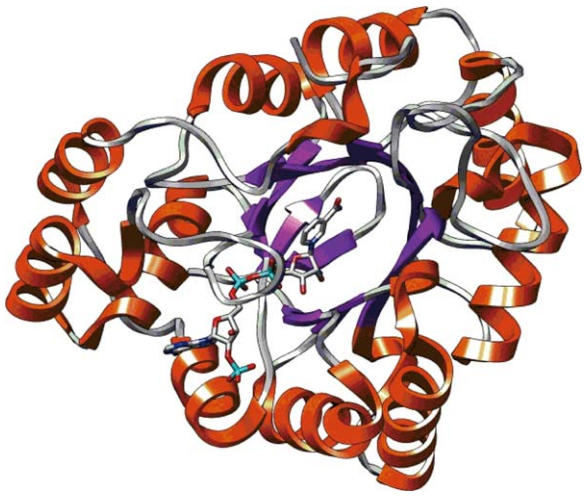

Fig. 1. The structure of aldose reductase.

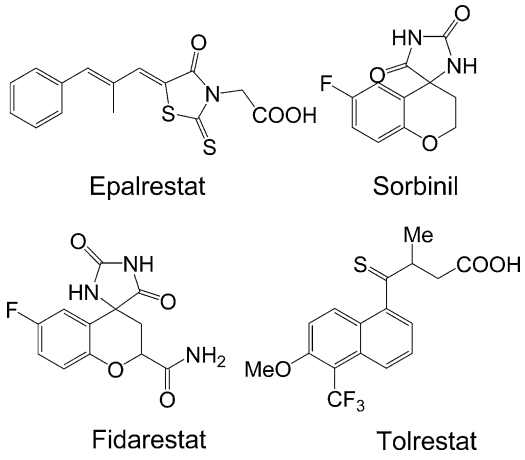

Fig. 2. Some orally active ALR2 inhibitors.

similar inhibitory activities. However, in vivo, the relative high p*K*a value and the concomitant advantage in pharmacokinetics make the spiro-hydantoin inhibitor Sorbinil prevail at both the inhibitory activity and the metabolite half-life. Despite of this, severe hypersensitivity reaction makes it impossible to be applied in clinical treatment [12,13]. To date, only Epalrestat is successfully marketed for treatment of diabetic neuropathy in Japan. Many products which appear to be promising during in vitro studies or in trials with animal models often fail to proceed any further because of undesirable side effects. These effects are mainly due to a lack of selectivity from other enzymes, especially the closely related aldehyde reductase (EC 1.1.1.2, ALR1), which has 51% identity in their amino acid sequences and plays a very important role in detoxification [7,13–15]. In recent years, a series of ARIs that are of high activities have been extracted from natural plants, such as flavones, flavonoids, coumarins and so on. Their medical value still needs to be further identified. Research on ARIs with high activity and specificity remains the focus of attention.

Although as early as 1986, compounds with anti-ALR2 activity had been isolated from *Dysidea* sp., *Ircinia ramose* and *Dactylospongia metachromia* sponge, however, the number of ARIs isolated from marine natural sources so far reported is still very limited [16–20]. Researches on marine ARIs are mainly focused on the extraction and separation of active ingredients, as well as activity detection. While, except for Fuente et al. [21] studied a series of polybrominated diphenyl ethers and their analogues through

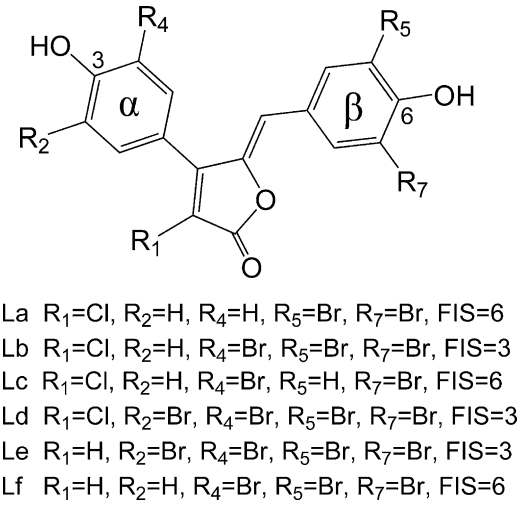

Fig. 3. Structures of the phenolic marine natural products, each FIS number gives the corresponding location of the first ionization site.

experimental and molecular docking methods, we find no other articles give the binding information of marine ARIs and ALR2. In a word, researches on the aspect of inhibitor–ALR2 binding mode and inhibition mechanism are far from satisfaction and urgently needed.

In recent years, a series of phenolic marine compounds were isolated from tunicates by Manzanaro et al. and had been experimentally proved to be ALR2-inhibitive [20]. But their binding modes with ALR2 and the inhibition mechanism are still unknown. Having structural similarities with coumarins we studied before [22], these compounds also share a central lactone group, but the phenolic inhibitors have one additional phenol group at each side of the 5-membered lactone ring (Fig. 3), which make them can bind with ALR2 through either the terminal phenolic hydroxyl group or the central lactone group. It is noteworthy that under the weak alkaline physiological environment in human body (pH ~ 7.4), the two terminal phenolic hydroxyls are probably ionized like flavones ARIs [12,23]. So in this paper, we performed automated docking and molecular dynamics studies on the neutral and ionized phenolic marine inhibitors with the aim to explore their interaction mode with ALR2, investigate their inhibitory mechanism and further provide some theoretical guidance to the research and development of new ARIs.

2. Methods

2.1. Model construction of enzyme and inhibitors

2.1.1. ALR2 enzyme preparation

Human aldose reductase-*h*ALR2 (PDB ID code: 2FZD) with high resolution 1.08 Å was downloaded from Brookhaven Protein Data Bank to serve as the docking acceptor [15]. The crystal structure is a complex of ARL2/$NADP^+$/Tolrestat. First, crystallographic waters were removed; then, the complex was optimized under Gromacs force field by performing 500 steps steepest descent energy minimization and a followed conjugate gradient energy minimization with a root-mean square criterion of the potential energy gradient of 0.01 kcal/mol/Å; finally, Tolrestat was deleted and the left ARL2/$NADP^+$ complex was used for docking experiment [21].

2.1.2. Inhibitor preparation

Quantum chemical software Gaussian 03 [24] was applied to optimize the structures of inhibitors at 6-31+G(d) basis set level by employing the Becke-3-parameter-Lee-Yang-Parr hybrid density

Table 1
Comparison of binding free energy[a] and inhibition constants calculated using Gasteiger and Mulliken atomic charges.

Phenolic marine ARIs	Gasteiger charge		Mulliken charge		Clog P[b]	Experimental IC_{50} (μM)
	Binding free energy[a] (kcal/mol)	Inhibition constant (μM)	Binding free energy (kcal/mol)	Inhibition constant (μM)		
La	−9.83	0.062	−7.01	7.31	5.22	0.8
La_ion1	−9.32	0.15	−7.32	4.32		
La_ion2	−8.84	0.33	−7.36	4.05		
Lb	−9.62	0.089	−6.62	13.97	6.10	12.7
Lb_ion1	−10.35	0.026	−7.46	3.37		
Lb_ion2	−10.01	0.046	−7.51	3.10		
Lc	−9.25	0.17	−6.80	10.31	5.41	16.9
Lc_ion1	−9.44	0.12	−6.89	8.95		
Lc_ion2	−9.78	0.068	−7.37	3.95		
Ld	−10.18	0.034	−6.88	9.10	6.79	18.7
Ld_ion1	−9.95	0.051	−7.39	3.80		
Ld_ion2	−10.57	0.018	−8.03	1.31		
Le	−9.10	0.22	−6.86	9.40	6.06	19.8
Le_ion1	−9.74	0.073	−7.71	2.24		
Le_ion2	−10.12	0.038	−8.11	1.13		
Lf	−8.55	0.54	−6.62	14.16	5.38	48.1
Lf_ion1	−9.16	0.19	−7.16	5.67		
Lf_ion2	−9.86	0.059	−7.97	1.43		

[a] Binding free energy = intermolecular energy + total internal energy + torsional free energy − unbound system's energy.
[b] The Clog P values are only for the neutral ligands.

functional theory (DFT). For each inhibitor, the conformation with the lowest energy was chosen as the docking ligand structure, the corresponding first and second ionized inhibitor conformations were derived based on the optimization of the neutral one. The first ionization state-FIS of each inhibitor was determined by comparing the electron densities on the 3-hydroxyl O and 6-hydroxyl O atom (Fig. 3). The hydroxyl O taking higher electron density forms relatively stronger interaction with its corresponding H, which make the hydroxyl harder to ionize, and vice versa. Apparently, on the ortho-sites of 3- or 6-hydroxyl, the Br substituent that bearing strong electron-withdrawing effect can effectively decreases the electron density of hydroxyl O atom, and make the ortho-hydroxyl more prone to ionization. The Clog P values describing the partition character between octanol and water were also calculated for all the neutral ligands (Table 1). It can be seen that, when increasing the substitution degree, Br substituent efficiently elevates the Clog P value, so that the corresponding ligand becomes more absorbable under physiological surroundings.

2.2. Automated docking setup

All the docking calculations were performed by using AutoDock 4.0 [25]. ALR2 enzyme was firstly modified by adding polar hydrogens and then kept rigid in docking process. While, all the torsional bonds of ligands were set free by Ligand module in AutoDock Tools-ADT. The docking area was defined by a box, centered on the Cα of the TRP111 residue. Grid points of $60 \times 60 \times 60$ with 0.375 Å spacing were calculated around the docking area for all the ligand atom types using AutoGrid. 50 separate docking calculations were performed for each ligand, each docking calculation consisted of the maximum 2.5×10^7 energy evaluations using the Lamarckian genetic algorithm local search method. For the local search, the Solis and Wets algorithm was applied using a maximum of 300 iterations. Each docking run was performed with a population size of 150. A mutation rate of 0.02 and a crossover rate of 0.8 were used to generate new docking trials for subsequent generations. The elitism value was set to 1. The docking results from each of the 50 calculations were clustered on the basis of root-mean square deviation (RMSD) between the Cartesian coordinates of the ligand atoms and were ranked according to the binding free energy. The structure with relative lower binding free energy and the most cluster members was chosen for the optimum docking conformation.

In docking calculation, the default Gasteiger partial atomic charges were used for ALR2 and the coenzyme $NADP^+$. While, for the inhibitors, the Gaussian 03 optimized Mulliken charges instead of the default Gasteiger ones were adopted, this is mainly due to these facts: (i) according to the function $IC_{50} = K_i(1 + S/K_m)$, the Mulliken inhibition constants have much better correlations with the experimental IC_{50} values compared to the Gasteiger inhibition constants that are all smaller than the experimental IC_{50} data by hundreds times (except for La) (Table 1). Where K_i is the inhibition constant calculated by AutoDock, S and K_m are the substrate concentration and the Michaelis–Menten constant of the substrate, respectively. Because the assays are performed under the same conditions, so both of S and K_m can be seen as constant, it is feasible to compare the K_i and the experimental IC_{50} values [11,26]; (ii) these two kinds of charges have slight influence on the docking conformations. The optimum docking results for each inhibitor almost have the same conformation in both cases; (iii) under Gasteiger charges, there is no consistent change trend of the binding free energies among three ionization states. While under Mulliken charges, the binding free energies of all inhibitors become more negative as the ionization proceeds, i.e., the binding of inhibitor and ALR2 becomes more and more stable. This result is consistent with the theory that under physiological conditions, the acidic groups such as phenolic hydroxyl should be ionized when binding to ALR2 [12,15,23].

2.3. Molecular dynamics setup

Molecular dynamics studies on Ligand/ALR2/$NADP^+$ system were carried out on the basis of molecular docking results by using Gromacs_3.3.1 software [27]. La and Lb, which showed the best experimental inhibition effects and represented two different binding modes, were taken to detailedly investigate the dynamical properties of the bound inhibitors.

The NPT ensemble and Gromacs force field were applied [22]. Each Ligand/ALR2/$NADP^+$ complex was placed in the center of a 72 Å × 72 Å × 72 Å cubic box and solvated by SPC/E water molecules, Na^+ counterions were added to keep the system

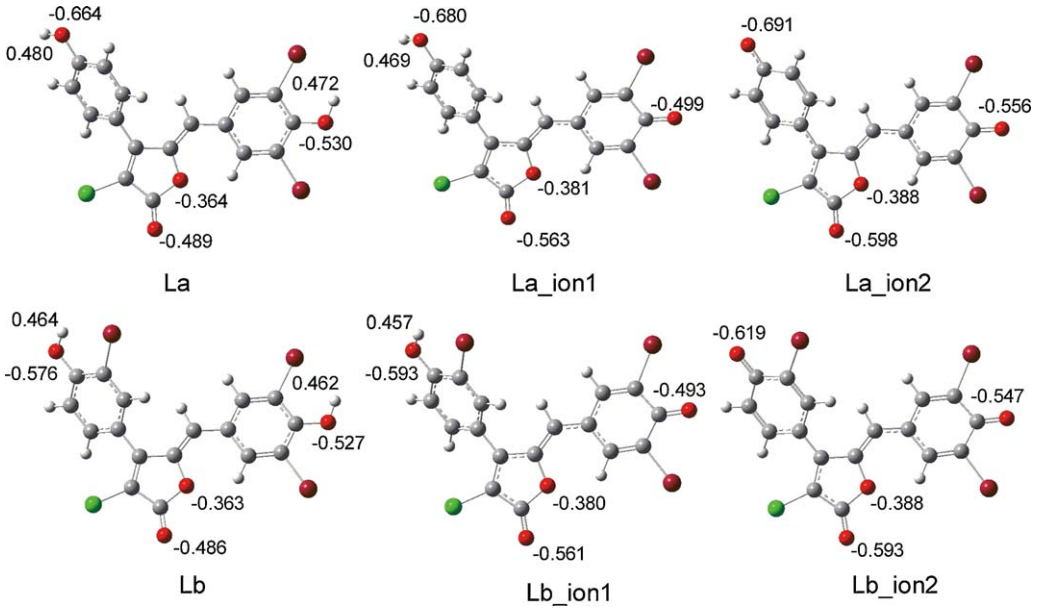

Fig. 4. Conformations of La and Lb at three different ionization states derived by Gaussian 03 optimization at B3LYP/6-31+G(d) level.

electrically neutral. Berendsen temperature and pressure coupling methods were applied to keep the system in stable environment (300 K, 1 Bar), both of the coupling constants were set 0.1. Particle mesh Ewald (PME) method for long-range electrostatics, a 9 Å cutoff for coulomb interaction, a 10 Å cutoff for van der Waals interactions, and the LINCS algorithm [28] for bond constraints were used. Each complex was firstly energy minimized using the steepest descent method; then, a 50 ps position restraining dynamics simulation was carried out by restraining the ARL2 with a 10 kJ/mol Å^2 harmonic constraint to relieve close contacts; finally, a 4 ns molecular dynamics simulation and subsequent result analysis were performed.

3. Results and discussion

3.1. Inhibitor conformations

Fig. 4 gives the optimal conformations of La, Lb and their ionized derivatives optimized by DFT method (conformations of the other inhibitors are shown in Supporting Information Fig. S1). For each conformation, the Mulliken charges of hydroxyl and lactone groups were labeled to study the ionization effect on the molecular structure and electron distribution. It is important to note that the conformation with the lowest energy should be selected, because on one hand, all of the inhibitors have perfect conjugate structures, so even slight conformational difference can cause remarkable change of the molecular charge distribution, which consequently affects the docking calculation; on the other hand, the torsion extent of the inhibitor conformation in docking results compared to the optimal one should be an assistant factor to judge the binding reasonableness. Apparently, a bigger conformational change corresponds to a higher energy barrier that the molecule needs to overcome.

3.2. Molecular docking

The 50 independent docking conformations for each inhibitor were clustered according to a 2.0 Å RMSD criterion. For La and Lb, the binding conformations of all their three ionization states and ALR2 are shown in Fig. 5 (the others are listed in Supporting Information Fig. S2). In order to clearly display the binding mode, residues that surround inhibitor beyond 5.0 Å and the coenzyme NADP$^+$ are not displayed.

It can be seen that, for every inhibitor, though the docking conformation changes, the polar group (phenol hydroxyl or lactone) that interact with the active residues of ALR2 does not alter as the inhibitor ionizes. The inhibitors can be divided into two classes according to their binding modes: (i) inhibitors that use the terminal phenol hydroxyl to form hydrogen bonds with active residues, such as La; (ii) inhibitors that bind with active residues through their lactone group, all the inhibitors except for La take this binding mode. The change of binding mode is probably caused by the substitution of the hydroxyl ortho H atoms with Br substituents which bring severe steric hindrance because of its big atomic volume. The structural characteristic is essential to the experimental inhibition activities of inhibitors, which vary a lot under these two binding modes (Table 1). This is probably because the hydroxyl O that bears more negative charges than the lactone carbonyl O can form more stable hydrogen bonds with active residues, which make the hydroxyl binding mode prevail at the binding strength; furthermore, compared to the carbonyl O which bears more severe steric effect (in a flat plane and connected with two big aromatic groups), the phenol hydroxyl that bonds with the five membered ring through the free rotational single bond can more effectively bind to the ALR2 active pocket.

Fig. 5A, B and C gives the docking conformations of La, La_ion1 and La_ion2, respectively. In three photos, all the inhibitors are hydrogen bonded with O$^{\eta}$H of TYR48 and N$^{\varepsilon 2}$H of HIS110 through their 3-hydroxyl O atoms, which make them anti-ALR2 active. Because just as reported, TYR48, HIS110 and TRP111 are the key residues that construct the active pocket [11–15,24]. The reason that the inhibitor binding group is the 3-hydroxyl instead of the 6-hydroxyl is that: the introduction of 5,7-Br substituent brings strong steric effect which makes the 6-hydroxyl incompatible with the active pocket.

As shown in Fig. 5A, there is an extra hydrogen bond between 6-hydroxyl O of La and O$^{\eta}$H of residue SER302, with the bond length of 2.03 Å. This ensures the β aromatic ring can stably anchor into the hydrophobic specialty pocket constructed by residues TRP111, PHE115, PHE122, TRP219, LEU300 and SER302. For inhibitor La_ion1, the hydrogen bond interaction with ALR2 is strongest judged by the hydrogen bond length (Fig. 5B). It has the lowest

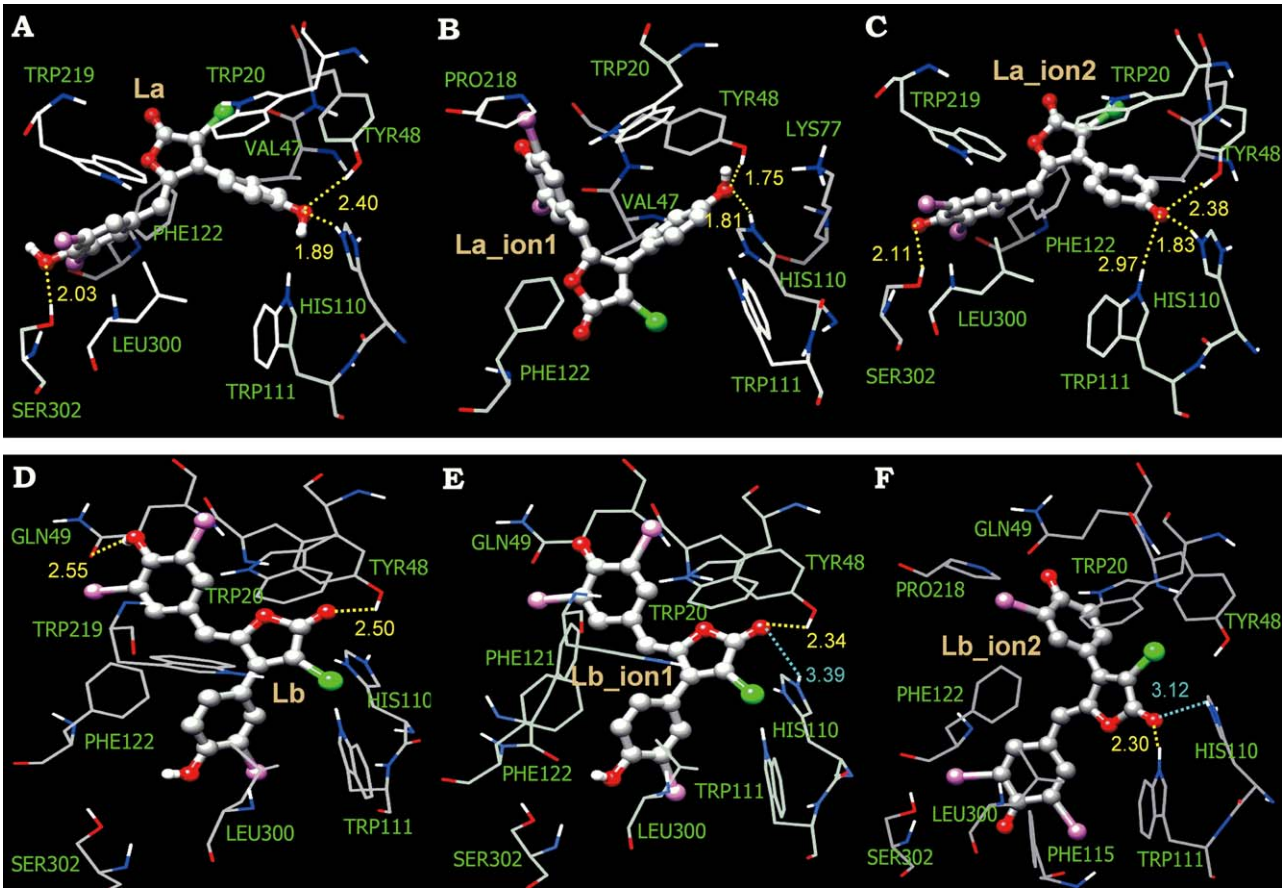

Fig. 5. Conformations of Ligand–ALR2 complexes derived by automated docking computation. For each ligand, the interaction of three ionization states and ALR2 are calculated and shown. The yellow dotted lines are used to represent proper hydrogen bonds, the cyan dotted lines are for the hydrogen bonds that the bond lengths are over 3.0 Å.

intermolecular energy (including van der Waals energy, hydrogen bonding energy, desolvation energy and electrostatic energy) among the three ionization states which is −7.91 kcal/mol. For La and La_ion2, the energies are −7.65 and −7.64 kcal/mol, respectively. But due to its severe conformational distortion compared to the optimal structure, La_ion1 does not have the lowest binding free energy (Table 1). Its torsional free energy reaches +0.82 kcal/mol, while for La and La_ion2, the values are +0.55 and +0.27 kcal/mol. Similar to La, the completely ionized La_ion2 also forms a hydrogen bond with the $O^{\eta}H$ of residue SER302 through the 6-hydroxyl O. More importantly, the ionized 3-hydroxyl O forms an additional hydrogen bond with $N^{\varepsilon 1}H$ of active residue TRP111 which increases the interaction strength of La_ion2 and ALR2 (Fig. 5C).

The docking conformations of Lb, Lb_ion1 and Lb_ion2 are given in Fig. 5D, E and F, respectively. It can be seen that both of Lb and Lb_ion1 are hydrogen bonded with TYR48 through the carbonyl O of lactone group. For Lb_ion1, there is an additional weak hydrogen bond with $N^{\varepsilon 2}H$ of HIS110, with the bond length of 3.39 Å. While for Lb_ion2, though hydrogen bonded with active residues through the same hydroxyl O atom, it has a reverse conformational orientation in the active site, i.e. the position of α ring of Lb_ion2 corresponds to the β ring of Lb and Lb_ion1, and vice versa. This reversal makes Lb_ion2 prefer to form hydrogen bonds with residues HIS110 and TRP111 rather than TYR48. As the ionization proceeding, the lengths of main hydrogen bonds (2.50 Å for Lb, 2.34 Å for Lb_ion1 and 2.30 Å for Lb_ion2) decrease, this means the interaction intensity of hydrogen bond between inhibitor and ALR2 increases gradually. It is notable that a hydrogen bond locates at the 6-hydroxyl H of Lb and the residue GLN49, this leads to the exposure of β aromatic ring to the apolar residues, such as VAL47 and TRP20, which is detrimental to binding stability. This hydrogen bond disappeared in Fig. 5E because of the ionization of 6-hydroxyl. While for Lb_ion2, the hydrogen bond was replaced by the new forming hydrogen bond which locates at the 6-hydroxyl O and the thiol H of CYS303. This transformation brings more stability for the hydrophobic interaction between the β ring and the specialty pocket, at the meantime, the docking free energy loss caused by conformational distortion decreased from +1.10 kcal/mol for Lb to +0.82 and +0.55 kcal/mol for Lb_ion1 and Lb_ion2, respectively. These two aspects indicate that the ionization of Lb can make the inhibitor-enzyme binding more stable and effective.

Inhibitors Lc–Lf and all their ionized derivatives are hydrogen bonded with active residues through carbonyl O atom. Except for Lc which take a reverse orientation, Lc_ion1, Lc_ion2 and all the other ligands anchor into the hydrophobic specialty pocket using the α aromatic ring (Supporting Information Fig. S2). Comparing the binding modes of the completely ionized inhibitors, it can be found that for Lc_ion2 and Ld_ion2, because the Cl substituent has strong electron-withdrawing ability and steric effect, hydrogen bonds mainly locate at $O^{\eta}H$ of TYR48, only very weak hydrogen bonds form with HIS110, with bond lengths of 3.50 and 3.44 Å, respectively. While for Le_ion2 and Lf_ion2, without the Cl substituent, they both can form strong hydrogen bonds with TYR48 and HIS110, which makes them have relatively larger binding free energies (Table 1).

Table 1 gives the binding free energies of all inhibitors at three ionization states. According to the changing trend of Mulliken

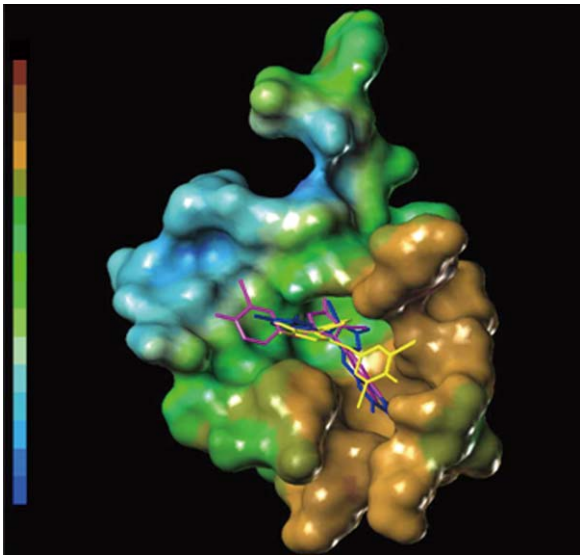

Fig. 6. Lipophilic potential surface constructed by all the residues that surround the ligands within 6.0 Å, as the color changes from brown to blue, the surface gradually becomes hydrophilic from hydrophobic. Three ligands are superposed in the active pocket, yellow for La_ion2, blue for Lb_ion2, and magenta for Lc_ion2.

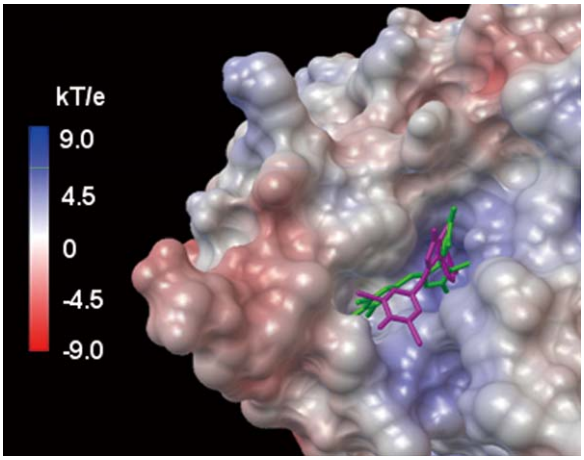

Fig. 7. APBS electrostatic potential, plotted on the surface of ALR2 enzyme from −9.0*kT*/*e* to 9.0*kT*/*e*. Where *k* is the Boltzmann constant, *T* is temperature, and *e* is the charge of electron. Two ligands are also shown in the surface, magenta for La_ion2, and green for Lb_ion2.

energies and related reports [12,15,23], the inhibitors should be ionized when binding with enzyme ALR2. In order to clearly identify the orientations of inhibitors in the whole catalysis area constituted by active pocket and specialty pocket, the docking conformations of entirely ionized inhibitors were superimposed in the lipophilic potential surface of ALR2, see Fig. 6 (because the positions and orientations of Ld_ion2, Le_ion2 and Lf_ion2 are highly identical with Lc_ion2, so only the first three inhibitors are shown). It can be seen that, 3-hydroxyl of La_ion2 anchors deeply into the green region which corresponds to the polar active residues. Although slightly differently oriented, both of Lb_ion2 and Lc_ion2 bind to the same polar region through the lactone group. It should be noted that the aromatic β ring of La_ion2 is completely embedded into the brown hydrophobic pocket, which makes it have potential good inhibition specialty. But for Lb_ion2, Lc_ion2 and all the other inhibitors, there is always one aromatic ring (α or β) extending into the green area mainly constituted by residues TRP20, VAL47 and GLN 49, which is unfavorable to the inhibition effectivity and binding stability.

For a better understanding of the role that the electrostatic effect plays in the binding of inhibitor–ALR2, the ALR2 APBS electrostatic potential was calculated (Fig. 7) [29]. It can be seen that the center of the active pocket is apparently light blue, indicating that this area has strong positive electrical property. Studies have revealed that the positive charges are mainly from the nicotinamide ring of $NADP^+$ and the protonated residues TYR48 and HIS110 [30–32], which makes the active pocket can steadily hold the inhibitors' polar groups that have partial negative charges through electrostatic interaction. For example, the 3-hydroxyl O of La_ion2 is deeply buried in the blue area, for Lb_ion2 and the other inhibitors, the whole lactone group and the negatively charged Cl substituent (if have) are all in the same area, which makes them have relatively stronger electrostatic interactions with the active pocket.

No good correlation was found by comparing the binding free energies and inhibition constants with the experimental IC_{50} values: the one has the highest binding free energy does not exhibit the best inhibition, and vice versa. This can be attributed to the fact that the intermolecular energy favorable lactone binding mode takes disadvantages at the hydrogen bond and hydrophobic interactions, which is more essential to the binding and inhibition effectivity.

3.3. Molecular dynamics

Molecular dynamics studies on La, Lb and their ionized derivatives are performed based on the docking results. The main purpose is to investigate the positional and conformational changes of inhibitors relative to the active pocket and the specialty pocket residues and further reveals the binding stability. After a 4 ns MD simulation for each inhibitor/ALR2/$NADP^+$ complex, the systems became equilibrated judged by their total energies' changing trends (Fig. S3). The RMSDs of inhibitor relative to ALR2 and ALR2 to its original conformation were calculated and outlined in Fig. 8. It can be seen that the enzymes become stable after 2 ns in all systems with a mean RMSD value of 2.0 Å.

Fig. 8A, B and C give the RMSDs of La, La_ion1 and La_ion2 relative to ALR2, respectively. La and La_ion2 have relatively smooth curves, their mean RMSD values are 1.7 and 3.0 Å. Actually, considering that the ALR2 itself has a 2.0 Å RMSD value, these two inhibitors should bind with enzyme very stably. This was confirmed by the examination of the interval conformations using VMD software, which displayed that the inhibitors were always anchored into the active site through the 3-hydroxyl O atom during the whole dynamic processes, and the RMSD values mainly correspond to the regular rotation of β aromatic ring around the single bond that connects β ring and the center 5-membered lactone ring. While for La_ion1, the RMSD value suddenly jumped from 2.0 to 4.3 Å at 1.25 ns, which implies a big conformational change of La_ion1 relative ALR2. But probably because of the strong hydrogen bond interaction of 3-hydroxyl O and residues TYR48 and HIS110, VMD showed that the binding group did not change. The unsmooth curve can be ascribed to the α and β ring partially overlapped binding conformation of La_ion1, which drives the β ring close to residue TRP20 and cannot be completely buried into the hydrophobic pocket like La and La_ion2.

RMSDs of lactone bound Lb, Lb_ion1 and Lb_ion2 are shown in parts D, E and F of Fig. 8. RMSD profiles of Lb and Lb_ion2 indicate that they both have dynamic stability. The RMSD curve of Lb mainly correlates with the rotation of 3-hydroxyl H and slightly positional change of β ring which partially extended into polar region. For La_ion2, its β ring anchors into the hydrophobic pocket and is fixed by the hydrogen bond located at 6-hydroxyl O and residue CYS303, which makes it do harmonious movement with ALR2 during the

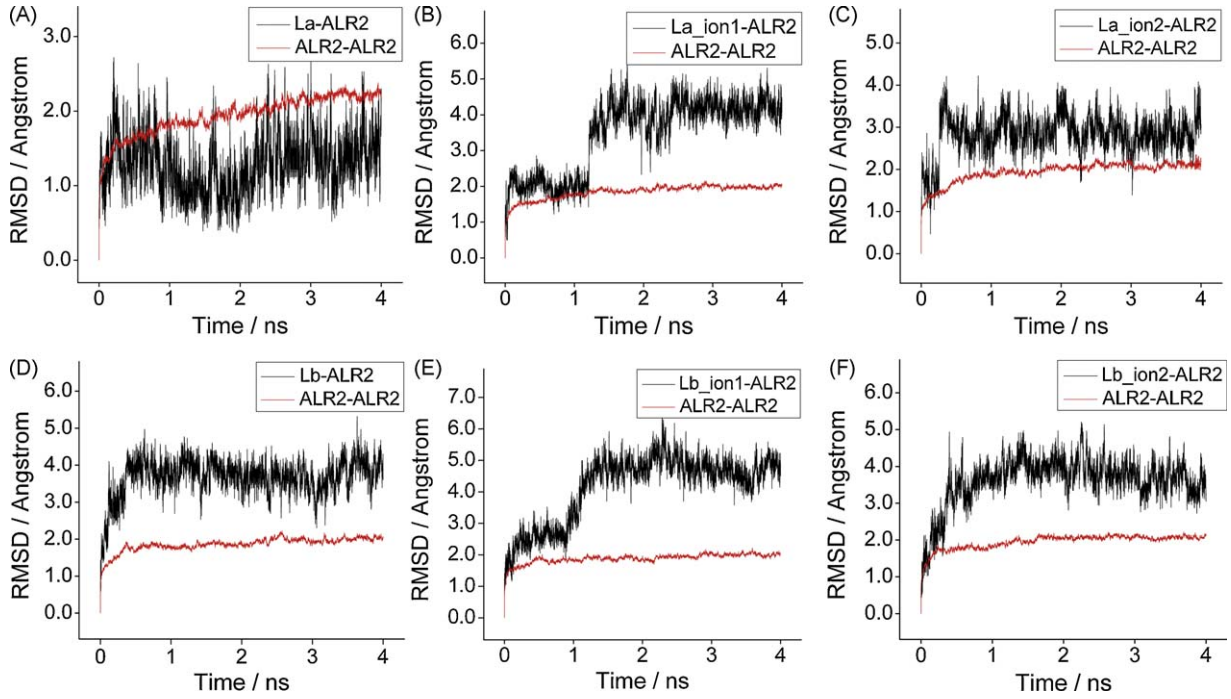

Fig. 8. RMSDs of La and Lb to ALR2 derived by dynamics calculation using Gromacs software. For each ligand, the three ionization states are considered. The RMSDs of ALR2 to itself are also presented by red lines.

whole dynamic process. Lb and Lb_ion2 have almost the same RMSD value which is 4.0 Å. As for inhibitor Lb_ion1, it has identical molecular orientation with Lb. But the ionization of 6-hydroxyl makes it cannot form hydrogen bond with residue GLN49 like Lb, which makes the methylene connected β ring bear more freedom in polar region. This is why the RMSD values gradually increased from 2.8 to 5.0 Å during 1.0–1.5 ns. But after the positional adjustment of β ring, Lb_ion1 stably binds with ALR2.

Molecular dynamic study shows that, though the lactone binding mode has relatively larger RMSD values compared to the 3-hydroxyl one, inhibitors under these two binding modes are dynamic steady. That is the reason that lactone bound Lb–Lf inhibitors displays stable experimental anti-ALR2 activities. It should be noticed that no matter which ionization state an inhibitor takes, the polar group used to form hydrogen bonds with active residues dose not change during the whole dynamic process.

3.4. Inhibition mechanism

Based on experimental and theoretical studies, it has been established that the reduction of an aldehyde substrate to an alcohol by ALR2 follows a stepwise mechanism, which consists of a hydride transfer from the nicotinamide ring of coenzyme NADPH and a proton transfer from one of the amino acid residues in the active site [30,33–37]. According to the residue mutation experiments, the most possible proton donors are TYR48 and protonated HIS110 [30,36,37].

In order to understand the inhibition mechanism of phenolic inhibitors, primary docking calculations were performed. The docking conformation of glucose–ALR2 shows that glucose mainly uses its carbonyl O atom to form hydrogen bonds with residues TYR48 and HIS110, which is much similar with the inhibitors' lactone binding mode. But glucose has much lower binding affinity compared with the inhibitors judged by its binding free energy (5.60 kcal/mol), which means ALR2 is probably more likely to bind with inhibitor molecules first. The docking calculation on glucose and inhibitor–ALR2 complex reveals that the glucose molecule can hardly enter into the active pocket and specialty pocket, because the whole area has been almost entirely occupied by the inhibitor molecule and cannot accommodate glucose any more, i.e. phenolic marine molecules inhibit ALR2 activities mainly by occupying the active space. Even glucose can enter the active site with inhibitor located at the binding site, our molecular docking and dynamics calculations have shown that all the phenolic marine inhibitors can form stable hydrogen bonds with TYR48 or HIS110 or both, which means the inhibitor can effectively hinder the proton transfer process and further stop the reduction reaction. More detailed studies are still deserved to further understand the inhibition mechanism.

4. Conclusion

On the basis of experimental data, our molecular docking and dynamics studies on phenolic marine natural ALR2 inhibitors reveals that they can form hydrogen bond networks with active residues by using the terminal hydroxyl or the center lactone carbonyl group; only when neither of the ortho-sites of the terminal hydroxyl is substituted by Br substituent (such as La), does an inhibitor adopt the hydroxyl binding mode. Otherwise, the inhibitor adopts the lactone binding mode. Both of the two binding modes are dynamic stable; for each inhibitor, the ionization dose not change the binding mode. But it does increase the binding free energies which reveal the importance of electrostatic interaction. Inhibitors exhibit their anti-ALR2 activities mainly by occupying the active site.

Under these two binding modes, phenolic marine inhibitors have different but stable experimental inhibition activities to *h*ALR2, and the binding mode alteration can be conveniently controlled by introducing or eliminating Br substituent on certain position of inhibitor molecules. These interesting characteristics make them a new kind of promising ALR2 inhibitors.

Acknowledgements

This work was supported by the National Natural Science Foundation of China (Nos. 30873158 and 20633060).

Appendix A. Supplementary data

Supplementary data associated with this article can be found, in the online version, at doi:10.1016/j.jmgm.2009.06.003.

References

[1] D. Wilson, K.M. Bohren, K.H. Gabbay, F.A. Quiocho, An unlikely sugar substrate site in the 1.65 A structure of the human aldose reductase holoenzyme implicated in diabetic complications, Science 257 (1992) 81–84.

[2] D.H. Harrison, K.M. Bohren, D. Ringe, G.A. Petsko, K.H. Gabbay, An anion binding site in human aldose reductase: mechanistic implications for the binding of citrate, cacodylate, and glucose 6-phosphate, Biochemistry 33 (1994) 2011–2020.

[3] D.R. Tomlinson, E.J. Stevens, L.T. Diemel, Aldose reductase inhibitors and their potential for the treatment of diabetic complications, Trends Pharmacol. Sci. 15 (1994) 293–297.

[4] P.F. Kador, The role of aldose reductase in the development of diabetic complications, Med. Res. Rev. 8 (1988) 325–352.

[5] C. Yabe-Nishimura, Aldose reductase in glucose toxicity: a potential target for the prevention of diabetic complications, Pharmacol. Rev. 50 (1998) 21–34.

[6] M. Brownlee, Biochemistry and molecular cell biology of diabetic complications, Nature 414 (2001) 813–820.

[7] T. Petrova, H. Steuber, I. Hazemann, A.C. Siah, A. Mitschler, R. Chung, M. Oka, G. Klebe, O.E. Kabbani, A. Joachimiak, A. Podjarny, Factorizing selectivity determinants of inhibitor binding toward aldose and aldehyde reductases: structural and thermodynamic properties of the aldose reductase mutant leu300Pro-fidarestat complex, J. Med. Chem. 48 (2005) 5659–5665.

[8] L. Costantino, G. Rastelli, M.C. Gamberini, D. Barlocco, Pharmacological approaches to the treatment of diabetic complications, Expert Opin. Ther. Pat. 10 (2000) 1245–1262.

[9] P.F. Kador, J.H. Kinoshita, N.E. Sharpless, Aldose reductase inhibitors: a potential new class of agents for the pharmacological control of certain diabetic complications, J. Med. Chem. 28 (1985) 841–849.

[10] G. Klebe, O. Kraemer, C. Sotriffer, Strategies for the design of inhibitors of aldose reductase, an enzyme showing pronounced induced-fit adaptations, Cell. Mol. Life. Sci. 61 (2004) 783–793.

[11] C. La Motta, S. Sartini, S. Salerno, F. Simorini, S. Taliani, A.M. Marini, F. Da Settimo, L. Marinelli, V. Limongelli, E. Novellino, Acetic acid aldose reductase inhibitors bearing a five-membered heterocyclic core with potent topical activity in a visual impairment rat model, J. Med. Chem. 51 (2008) 3182–3193.

[12] L. Costantino, G. Rastelli, M.C. Gamberini, J.A. Vinson, P. Bose, A. Iannone, M. Staffieri, L. Antolini, A. Del Corso, U. Mura, A. Albasini, 1-Benzopyran-4-one antioxidants as aldose reductase inhibitors, J. Med. Chem. 42 (1999) 1881–1893.

[13] G. Rastelli, A.M. Ferrari, L. Costantino, M.C. Gamberini, Discovery of new inhibitors of aldose reductase from molecular docking and database screening, Bioorg. Med. Chem. 10 (2002) 1437–1450.

[14] F. Da Settimo, G. Primofiore, C. La Motta, S. Sartini, S. Taliani, F. Simorini, A.M. Marini, A. Lavecchia, E. Novellino, E. Boldrini, Naphtho[1,2-*d*]isothiazole acetic acid derivatives as a novel class of selective aldose reductase inhibitors, J. Med. Chem. 48 (2005) 6897–6907.

[15] C. La Motta, S. Sartini, L. Mugnaini, F. Simorini, S. Taliani, S. Salerno, A.M. Marini, F. Da Settimo, A. Lavecchia, E. Novellino, M. Cantore, P. Failli, M. Ciuffi, Pyrido[1,2-*a*]pyrimidin-4-one derivatives as a novel class of selective aldose reductase inhibitors exhibiting antioxidant activity, J. Med. Chem. 50 (2007) 4917–4927.

[16] M. Sugano, A. Sato, H. Nagak, S. Yoshioka, T. Shiraki, H. Horikoshi, An improved variant of the julia olefin synthesis: reductive elimination of β-hydroxy imidazolyl sulfones by samarium dhodide, Tetrahedron Lett. 31 (1990) 7015–7108.

[17] A. Sato, T. Morishita, T. Shiraki, S. Yoshioka, H. Horikoshi, H. Kuwano, H. Hanzawa, T. Hata, Aldose reductase inhibitors from a marine sponge, dictyodendrilla sp., J. Org. Chem. 58 (1993) 7632–7634.

[18] H. Nakamura, S. Yamaguchi, T. Hayashi, M. Baba, Y. Okada, J. Tanaka, H. Tokuda, H. Nishino, T. Okuyama, Studies on the biological activities of marine algae (III) Antitumor promoting activity and inhibitory effect on aldose reductase, Nat. Med. 51 (1997) 162–169.

[19] J.Á. De La Fuente, S. Manzanaro, Aldose reductase inhibitors from natural sources, Nat. Prod. Rep. 20 (2003) 243–251.

[20] S. Manzanaro, J. Salvá, J.Á. De la Fuente, Phenolic marine natural products as aldose reductase inhibitors, J. Nat. Prod. 69 (2006) 1485–1487.

[21] J.Á. De La Fuente, S. Manzanaro, M.J. Martín, T.G. De Quesada, I. Reymundo, S.M. Luengo, F. Gago, Synthesis, activity, and molecular modeling studies of novel human aldose reductase inhibitors based on a marine natural product, J. Med. Chem. 46 (2003) 5208–5221.

[22] Z. Wang, B. Ling, R. Zhang, Y. Liu, Docking and molecular dynamics study on the inhibitory activity of coumarins on aldose reductase, J. Phys. Chem. B 112 (2008) 10033–10040.

[23] L. Costantino, G. Rastelli, K. Vescovini, G. Cignarella, P. Vianello, A. Del Corso, M. Cappiello, U. Mura, D. Barlocco, Synthesis, activity, and molecular modeling of a new series of tricyclic pyridazinones as selective aldose reductase inhibitors, J. Med. Chem. 39 (1996) 4396–4405.

[24] M.J. Frisch, G.W. Trucks, H.B. Schlegel, G.E. Scuseria, M.A. Robb, J.R. Cheeseman, J.A. Montgomery Jr., T. Vreven, K.N. Kudin, J.C. Burant, J.M. Millam, S.S. Iyengar, J. Tomasi, V. Barone, B. Mennucci, M. Cossi, G. Scalmani, N. Rega, G.A. Petersson, H. Nakatsuji, M. Hada, M. Ehara, K. Toyota, R. Fukuda, J. Hasegawa, M. Ishida, T. Nakajima, Y. Honda, O. Kitao, H. Nakai, M. Klene, X. Li, J.E. Knox, H.P. Hratchian, J.B. Cross, V. Bakken, C. Adamo, J. Jaramillo, R. Gomperts, R.E. Stratmann, O. Yazyev, A.J. Austin, R. Cammi, C. Pomelli, J.W. Ochterski, P.Y. Ayala, K. Morokuma, G.A. Voth, P. Salvador, J.J. Dannenberg, V.G. Zakrzewski, S. Dapprich, A.D. Daniels, M.C. Strain, O. Farkas, D.K. Malick, A.D. Rabuck, K. Raghavachari, J.B. Foresman, J.V. Ortiz, Q. Cui, A.G. Baboul, S. Clifford, J. Cioslowski, B.B. Stefanov, G. Liu, A. Liashenko, P. Piskorz, I. Komaromi, R.L. Martin, D.J. Fox, T. Keith, M.A. Al-Laham, C.Y. Peng, A. Nanayakkara, M. Challacombe, P.M.W. Gill, B. Johnson, W. Chen, M.W. Wong, C. Gonzalez, J.A. Pople, Gaussian 03, Revision C.02, Gaussian, Inc., Wallingford, CT, 2004.

[25] G.M. Morris, D.S. Goodsell, R.S. Halliday, R. Huey, W.E. Hart, R.K. Belew, A.J. Olson, Automated docking using a Lamarckian genetic algorithm and an empirical binding free energy function, J. Comput. Chem. 19 (1998) 1639–1662.

[26] Y. Cheng, W.H. Prusoff, Relationship between the inhibition constant (K_I) and the concentration of inhibitor which causes 50 per cent inhibition (I_{50}) of an enzymatic reaction, Biochem. Pharmacol. 22 (1973) 3099–3108.

[27] D. Van Der Spoel, E. Lindahl, B. Hess, G. Groenhof, A.E. Mark, H.J. Berendsen, GROMACS: fast, flexible and free, J. Comput. Chem. 26 (2005) 1701–1718.

[28] B. Hess, J. Bekker, H.J.C. Berendsen, J.G.E.M. Fraaije, LINCS: a linear constraint solver for molecular simulations, J. Comput. Chem. 18 (1997) 1463–1472.

[29] N.A. Baker, D. Sept, S. Joseph, M.J. Holst, J.A. McCammon, Electrostatics of nanosystems: application to microtubules and the ribosome, Proc. Natl. Acad. Sci. 98 (2001) 10037–10041.

[30] P. Várnai, W.G. Richards, P.D. Lyne, Modelling the catalytic reaction in human aldose reductase, Proteins 37 (1999) 218–227.

[31] Y.S. Lee, M. Hodoscek, P.F. Kador, K. Sugiyama, Hydrogen bonding interactions between aldose reductase complexed with NADP(H) and inhibitor tolrestat studied by molecular dynamics simulations and binding assay, Chem. Biol. Interact. 143–144 (2003) 307–316.

[32] I.T. Suydam, C.D. Snow, V.S. Pande, S.G. Boxer, Electric fields at the active site of an enzyme: direct comparison of experiment with theory, Science 313 (2006) 200–204.

[33] K.M. Bohren, C.E. Grimshaw, C.J. Lai, D.H. Harrison, D. Ringe, G.A. Petsko, K.H. Gabbay, Tyrosine-48 is the proton donor and histidine-110 directs substrate stereochemical selectivity in the reduction reaction of human aldose reductase: enzyme kinetics and crystal structure of the Y48H mutant enzyme, Biochemistry 33 (1994) 2021–2032.

[34] C.E. Grimshaw, K.M. Bohren, C.J. Lai, K.H. Gabbay, Human aldose reductase: subtle effects revealed by rapid kinetic studies of the C298A mutant enzyme, Biochemistry 34 (1995) 14366–14373.

[35] C.E. Grimshaw, K.M. Bohren, C.J. Lai, K.H. Gabbay, Human aldose reductase: pK of tyrosine 48 reveals the preferred ionization state for catalysis and inhibition, Biochemistry 34 (1995) 14374–14384.

[36] Y.S. Lee, M. Hodoscek, B.R. Brooks, P.F. Kador, Catalytic mechanism of aldose reductase studied by the combined potentials of quantum mechanics and molecular mechanics, Biophys. Chem. 70 (1998) 203–216.

[37] P. Várnai, A. Warshel, Computer simulation studies of the catalytic mechanism of human aldose reductase, J. Am. Chem. Soc. 122 (2000) 3849–3860.